

tive" capture through the giant dipole resonance results in a peak in the cross sections at about 15 MeV.

Figure 6 shows the  $(n,\gamma)$  cross-section measurements of this experiment compared with the theoretical predictions of Lane and Lynn<sup>6</sup> and Brown.<sup>9</sup> The dashed curve (a) corresponds to Lane and Lynn's simplified direct-capture cross section [Eq. (1)] and the solid curve (b) corresponds to curve (a) multiplied by Brown's enhancement factor  $F$  [Eq. (2)]. The magnitude of  $F$  is quite sensitive to the half-width  $\Gamma_D$  of the giant dipole resonance, and only approximate values of these half-widths are obtained from the  $(\gamma,n)$  cross-section curves. The photoneutron cross sections of  $\text{Mn}^{55}$  and  $\text{Ho}^{165}$  show a splitting of the giant dipole resonance caused by the intrinsic deformation of these nuclides. For example, high-resolution measurements<sup>40,41</sup> of the  $(\gamma,n)$  cross section of  $\text{Ho}^{165}$  show two peaks with the

following parameters:  $E_{D_1}=12.3$  MeV,  $\Gamma_{D_1}=2.5$  MeV and  $E_{D_2}=15.7$  MeV,  $\Gamma_{D_2}=4.4$  MeV. In the calculation of  $F$ ,  $\Gamma_D$  was taken as the sum of the two separate half-widths and  $E_D$  was taken as the average of the two peak energies.

In comparing the calculated curves with the measurements, it can be seen that the enhancement factor is needed for all of the cases, and the magnitude and shape of the calculated cross sections are in reasonable agreement with the measurements. The agreement between the calculated and measured cross sections of  $\text{Na}^{23}$  and  $\text{Mn}^{55}$  must be rather fortuitous since errors of a factor of 4 in the theoretical predictions would not be unreasonable according to Refs. 8–10. The theoretical predictions for the activation of  $\text{In}^{116m}$  and  $\text{Ho}^{166}$  have not been reduced from values given by Eqs. (1) and (2) to take into account the production of  $\text{In}^{116g}$  and  $\text{Ho}^{166m}$ .

### Activation Cross Sections for the $\text{F}^{19}(n,2n)\text{F}^{18}$ , $\text{Na}^{23}(n,2n)\text{Na}^{22}$ , $\text{Mn}^{55}(n,2n)\text{Mn}^{54}$ , $\text{In}^{115}(n,2n)\text{In}^{114m}$ , $\text{Ho}^{165}(n,2n)\text{Ho}^{164m}$ , $\text{In}^{115}(n,n')\text{In}^{115m}$ , and $\text{Al}^{27}(n,\alpha)\text{Na}^{24}$ Reactions\*

H. O. MENLOVE,<sup>†</sup> K. L. COOP,<sup>‡</sup> AND H. A. GRECH  
*Lockheed Palo Alto Research Laboratory, Palo Alto, California*

AND

R. SHER  
*Stanford University, Stanford, California*  
 (Received 29 June 1967)

The  $(n,2n)$  activation cross sections of  $\text{F}^{19}$ ,  $\text{Na}^{23}$ ,  $\text{Mn}^{55}$ ,  $\text{In}^{115}$ , and  $\text{Ho}^{165}$  have been measured in the neutron energy range from 12.7 to 19.4 MeV. In addition, the activation cross sections for the  $\text{In}^{115}(n,n')\text{In}^{115m}$  and  $\text{Al}^{27}(n,\alpha)\text{Na}^{24}$  reactions have been measured in the energy range from 1.0 to 19.4 MeV and from 6.1 to 19.4 MeV, respectively. Most of the measurements were made relative to the fission cross section of  $\text{U}^{235}$ . The experimental  $(n,2n)$  cross sections have been compared with the predictions of the semiempirical cross-section theories of Pearlstein and of Gardner.

#### INTRODUCTION

**A** KNOWLEDGE of the shape and magnitude of  $(n,2n)$  and  $(n,n')$  cross sections as a function of neutron energy is of interest from the standpoint of nuclear-reaction theory and in connection with the use of certain materials as threshold detectors and neutron-flux-measuring standards.

In the present experiment,  $(n,2n)$  activation cross sections of  $\text{F}^{19}$ ,  $\text{Na}^{23}$ ,  $\text{Mn}^{55}$ ,  $\text{In}^{115}$ , and  $\text{Ho}^{165}$  have been

measured in the neutron energy range from 12.7 to 19.4 MeV. Also, the  $(n,n')$  activation cross section of  $\text{In}^{115}$  has been measured in the neutron energy range from 1.0 to 19.4 MeV. At most energies, all these cross sections were measured relative to the  $\text{U}^{235}(n,f)$  cross section. These particular nuclides were studied since they were activated in these ways in conjunction with the  $(n,\gamma)$  cross-section measurements described in a companion paper.<sup>1</sup> In addition, the convenient decay schemes and half-lives of the product nuclides make these reactions possible candidates for use as threshold detectors. The  $\text{In}^{115}(n,n')\text{In}^{115m}$  reaction is especially useful in this regard because of its low threshold (0.34 MeV) and convenient half-life (4.5 h).

\* This work supported by the Lockheed Independent Research Program and is based on part of a thesis submitted by H. O. Menlove to Stanford University in partial fulfillment of the requirements for the Ph.D. degree.

<sup>†</sup> Present address: Los Alamos Scientific Laboratory, University of California, Los Alamos, New Mexico.

<sup>‡</sup> Present address: Department of Nuclear Physics, Research School of Physical Sciences, Australian National University, Canberra.

<sup>1</sup> H. O. Menlove, K. L. Coop, H. A. Grech, and R. Sher, *Phys. Rev.* **163**, 1308 (1967).

TABLE I. Information concerning the investigated nuclides.

Reaction	Half-life	Counting crystal <sup>a</sup> (in.)	Counting interval (keV)	$\gamma$ -ray energy <sup>b</sup> (MeV)	$\gamma$ rays per decay of nuclide <sup>c</sup>
$F^{19}(n,2n)F^{18}$	1.83 h	4×4	430–590	0.511	1.94
$Na^{23}(n,2n)Na^{22}$	2.62 yr	4×4	1720–1990	1.278	1.00
$Mn^{55}(n,2n)Mn^{54}$	313.5 d	3×3	720–960	0.835	1.00
$In^{115}(n,2n)In^{114m}$	50.0 d	2×2	150–245	0.191	0.173
$Ho^{165}(n,2n)Ho^{164m}$	39 min	1.75×0.25	39–80	... <sup>d</sup>	... <sup>d</sup>
$In^{115}(n,n')In^{115m}$	4.50 h	2×2	285–400	0.335	0.50
$Al^{27}(n,\alpha)Na^{24}$	15.05 h	3×3	1240–1520	2.753	1.00

<sup>a</sup> Dimensions of the cylindrical NaI(Tl) crystal used to count the sample.  
<sup>b</sup> Energy of  $\gamma$  ray used to determine the decay rate.

<sup>c</sup> Branching ratios obtained from Ref. 5.  
<sup>d</sup> Counting efficiency not used in cross-section calculations.

Samples of aluminum were also irradiated in this experiment to make possible the measurement of the  $Al^{27}(n,\alpha)Na^{24}$  cross section. Since this cross section is relatively well known, its measurement in this experiment served as a check on the fission-chamber calibration. In addition, the  $Al^{27}(n,\alpha)Na^{24}$  reaction has a threshold energy of 3.3 MeV, and so it cannot be produced by low-energy background neutrons. On the other hand, the  $(n,f)$  cross section of  $U^{235}$  is much larger for low-energy neutrons than it is for high-energy neutrons; hence, the presence of low-energy background neutrons that are not properly corrected for would probably make the  $(n,\alpha)$  cross sections of Al measured in this experiment deviate from the published values.<sup>2</sup>

Activation techniques were used to determine the number of interactions occurring in the samples during the neutron irradiations, and  $\gamma$ -ray counting techniques were usually employed to normalize the relative values of the cross sections. A different technique was used for  $Ho^{165}(n,2n)Ho^{164m}$  where a direct normalization of the cross section was made to the results of other work done at 14 MeV.

The energy dependences and magnitudes of the  $(n,2n)$  cross sections obtained from the present experiment have been compared with calculated results based on the semiempirical cross-section theories of Pearlstein<sup>3</sup> and of Gardner<sup>4</sup> to help evaluate the usefulness of these theories.

### EXPERIMENTAL PROCEDURES

Since most of the experimental procedures have been described in detail in the companion paper<sup>1</sup> on the  $(n,\gamma)$  cross-section measurements, only a summary of the procedures will be given here. The target samples, neutron-production reactions, irradiation geometry and procedures, and neutron-flux measurements were the same as those described in the preceding paper.<sup>1</sup> However, since the  $(n,2n)$ ,  $(n,n')$ , and  $(n,\alpha)$  reactions are

of the threshold type, they cannot be produced by low-energy background neutrons, and the contribution to the sample activity from scattered neutrons was usually negligible. The irradiations at neutron energies of 12.7, 12.9, and 13.3 MeV were carried out with the samples at back angles. At 12.7 and 12.9 MeV, the fission counter could not be positioned closely enough to the neutron source to achieve sufficient activity in the samples, and so it was not used. Cross sections at these two energies were therefore obtained relative to the  $Al^{27}(n,\alpha)Na^{24}$  cross section.

After the irradiations, the activated samples were counted on four NaI(Tl) crystals which were coupled to four 100-channel sections of a pulse-height analyzer. Table I lists the reactions for which the cross sections were measured, the half-lives<sup>5</sup> of the induced activities, and the energy intervals that were followed in order to determine the number of interactions that occurred during the neutron irradiation. The pulse-height spectra from each sample were generally collected for a period of several half-lives so that the decay of the sample could be analyzed. This decay was analyzed using a least-squares exponential-decay computer program. Because of the long half-lives of  $Na^{22}$  (2.62 y) and  $Mn^{54}$  (314 d), these decays were followed for only a fraction of their half-lives. The decay of  $In^{115m}$  (4.5 h) was not analyzed for the first 4 or 5 h after the end of an irradiation because of the presence of interfering  $\gamma$  rays from the  $In^{116m}$  (54 min) and  $In^{118m}$  (1.73 h) decays. The target samples were counted on the NaI(Tl) crystals which were mentioned in the companion paper.<sup>1</sup>

In order to obtain the efficiencies for counting the activated samples, the samples were irradiated in an intense 15.0-MeV neutron flux and then counted at 15.2-cm above a carefully calibrated<sup>6</sup> 4×4-in. NaI(Tl) crystal which was covered by a 0.75-g/cm<sup>2</sup>  $\beta$ -ray absorber. Table I lists the energy of the  $\gamma$  ray that was used to determine the decay rate, and the number<sup>5</sup> of  $\gamma$  rays per decay of the nuclide. With the exception of the details described below, the calibration procedures were the same as those described in the previous paper.<sup>1</sup>

<sup>2</sup> *Neutron Cross Sections*, compiled by J. R. Stehn, M. D. Goldberg, B. A. Magurno, and R. Wiener-Chasman, Brookhaven National Laboratory Report No. 325 (U. S. Government Printing and Publishing Office, Washington, D. C., 1958), 2nd ed., Suppl. 2, Vol. I.

<sup>3</sup> S. Pearlstein, Nucl. Sci. Eng. 23, 238 (1965).

<sup>4</sup> D. G. Gardner, Lawrence Radiation Laboratory Report No. UCRL-14575 (unpublished).

<sup>5</sup> *Nuclear Data Sheets*, compiled by K. Way *et al.* (Printing and Publishing Office, National Academy of Sciences-National Research Council, Washington, D. C., 1958-64).

<sup>6</sup> K. L. Coop and H. A. Grench, Nucl. Instr. Methods 36, 339 (1965).

TABLE II. The  $(n,2n)$  activation-cross-section results.

Neutron energy <sup>a</sup> (MeV)	One-half full energy spread (MeV)	F <sup>19</sup> $(n,2n)$ F <sup>18</sup> (mb)	Na <sup>23</sup> $(n,2n)$ Na <sup>22</sup> (mb)	Mn <sup>55</sup> $(n,2n)$ Mn <sup>54</sup> (mb)	In <sup>115</sup> $(n,2n)$ In <sup>114m</sup> (mb)	Ho <sup>165</sup> $(n,2n)$ Ho <sup>164m</sup> (mb)
12.70	0.36	16.3±1.6 <sup>b</sup>	...	546±51 <sup>b</sup>	1054±119 <sup>b</sup>	1041±117 <sup>b</sup>
12.94	0.68	22.8±2.3	...	583±54	1162±130	1017±114
13.28	0.61	26.4±2.6	...	658±61	1021±115	940±105
13.50	0.47	30.5±3.7	12.0±10.0 <sup>b</sup>	613±72	1007±138	1005±142
14.96	0.87	60.8±6.0	43.1± 6.4	854±79	1264±137	1050±117
15.82	0.45	71.4±7.0	50.6±13.2	890±82	1325±144	1047±117
16.52	0.35	78.9±7.7	79.7±11.6	906±84	1278±140	1042±116
17.35	0.32	90.5±9.5	87.0±18.6	910±85	1252±137	877± 98
18.44	0.33	90.2±9.0	90.9±10.9	887±82	1139±124	670± 75
19.39	0.35	85.4±8.4	99.1±11.8	822±76	1040±113	476± 53

<sup>a</sup> Laboratory system.<sup>b</sup> Uncertainty in absolute value of the cross section.

In counting the F<sup>18</sup>(1.83 h) activity, the NaF sample was completely surrounded by 0.19 cm of Lucite in order to insure the annihilation of the 0.65-MeV positrons in the immediate vicinity of the NaF sample. Secondly, the Na<sup>22</sup>(2.62 yr) activity was too weak to count 15.2-cm above the crystal, and so a calibrated Na<sup>22</sup> source obtained from the National Bureau of Standards was used to determine the counting efficiency in close geometry. The standard Na<sup>22</sup> point source was counted above and below a nonactivated NaF target sample, and the average of these two counting rates was used to determine the counting efficiency. The top of the NaF disk was covered with a 0.25-cm-thick layer of Lucite to insure the annihilation of the 0.54-MeV positron in the immediate vicinity of the NaF sample.

At the time the present cross-section measurements were made, only one Ho<sup>164</sup> activity had been established, although there was some evidence<sup>5</sup> that two states of about the same half-life exist. More recent information

confirms that there are indeed two activities, Ho<sup>164m</sup>( $T_{1/2} = 37.5_{-0.5}^{+1.5}$ , Ref. 7;  $T_{1/2} = 39.0 \pm 0.5$  min, Ref. 8) and Ho<sup>164g</sup>( $T_{1/2} = 29 \pm 2$  min, Ref. 7;  $T_{1/2} = 23.9 \pm 0.5$  min, Ref. 8). In the present experiments, the activated Ho sample was counted on the thin Al window of a 1.75-in.-diam.  $\times$  0.25-in. NaI(Tl) crystal. The counting interval included the region from 39 to 80 keV, and the decay of the activity was analyzed, using the least-squares exponential-decay computer program. In retrospect, this counting interval favored strongly<sup>8</sup> the counting of Ho<sup>164m</sup> over Ho<sup>164g</sup>.

## RESULTS AND DISCUSSION

### Comparisons with Other Experimental Results

The cross-section measurements were corrected for the same effects as mentioned in the companion paper.<sup>1</sup> However, as mentioned above, no correction was necessary for low-energy background neutrons. The corrections for scattered neutrons were negligible for the  $(n,2n)$  reactions and they were usually small (<5%) for the  $(n,n')$  and  $(n,\alpha)$  reactions.

Other sources of error which affect the shapes of the cross-section curves are as follows (all quoted uncertainties are in terms of standard deviations): (a) counting statistics and electronic gain shifts ( $\pm 1\%$ , except for Na<sup>22</sup>, for which the uncertainty was  $\pm 2$ – $20\%$ ), (b) uncertainty in the ratio of the intensity of the second neutron group from the Be<sup>9</sup> $(\alpha,n)$ C<sup>12</sup> reaction to that of the higher-energy group ( $\pm 1\%$ ), and (c) incorrect shape of the U<sup>235</sup> fission cross section used for normalization (<5%). Uncertainties in the following factors equally affect all cross sections for a particular nuclide, regardless of the neutron energy: (a) the decay schemes [negligible except for the cases of In<sup>114m</sup>(50 d) and In<sup>115m</sup>(4.5 h) where the errors were  $\pm 4$  and  $\pm 2.6\%$ , respectively], (b) fitting a Gaussian curve to the photopeak ( $\pm 1$ – $2\%$ ), (c) relative counting efficiency of the calibrated NaI(Tl) crystal for the  $\gamma$  ray involved and the 0.412-MeV  $\gamma$  ray of Au<sup>198</sup>( $\pm 1$ – $2.5\%$ ), (d) the posi-

TABLE III. Activation cross sections for the In<sup>115</sup> $(n,n')$ In<sup>115m</sup> and the Al<sup>27</sup> $(n,\alpha)$ Na<sup>24</sup> reactions.

Neutron energy <sup>a</sup> (MeV)	One-half full energy spread (MeV)	In <sup>115</sup> $(n,n')$ In <sup>115m</sup> (mb)	Al <sup>27</sup> $(n,\alpha)$ Na <sup>24</sup> (mb)
0.97	0.10	69.7± 9.5 <sup>b</sup>	...
1.56	0.12	187 ±26	...
2.15	0.13	317 ±29	...
3.27	0.52	342 ±31	...
3.57	0.29	343 ±31	...
4.00	0.24	351 ±32	...
4.58	0.23	355 ±33	...
5.39	0.25	354 ±36	...
6.13	0.28	334 ±34	2.24± 0.22 <sup>b</sup>
8.06	0.14	294 ±36	38.2 ± 3.8
12.70	0.36	102 ±11	...
12.94	0.68	101 ±11	...
13.28	0.61	78.9± 8.1	116 ±11
13.50	0.47	80.9±10.2	116 ±14
14.96	0.87	61.6± 6.3	111 ±11
15.82	0.45	59.2± 6.4	104 ±10
16.52	0.35	59.4± 6.1	89.3 ± 8.7
17.35	0.32	57.4± 5.9	71.0 ± 7.0
18.44	0.33	55.4± 6.0	51.2 ± 5.0
19.39	0.35	55.6± 5.7	39.1 ± 3.9

<sup>a</sup> Laboratory system.<sup>b</sup> Uncertainty in absolute value of the cross section.<sup>7</sup> M. H. Jorgensen, O. B. Nielsen, and D. Skilbreid, Nucl. Phys. 84, 569 (1966).<sup>8</sup> B. Sethi and S. K. Mukherjee, Nucl. Phys. 85, 227 (1966).

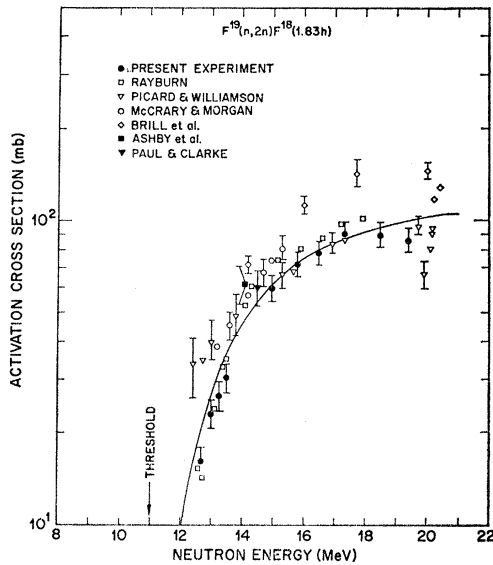


FIG. 1. The  $F^{19}(n,2n)F^{18}$  activation cross section. The curve corresponds to the theoretical predictions of Pearlstein and of Gardner normalized to the cross-section measurements of this experiment.

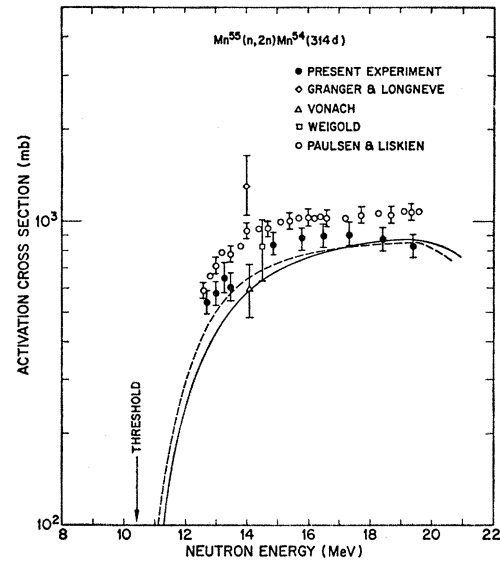


FIG. 3. The  $Mn^{55}(n,2n)Mn^{54}$  activation cross section. The solid curve corresponds to the theoretical predictions of Pearlstein, and the dashed curve corresponds to the theoretical predictions of Gardner.

tion of the samples relative to the fission foil ( $\pm 0.5$ – $1.5\%$ ), and (e) the absolute values of the  $(n,f)$  cross section of  $U^{235}$  ( $\pm 5\%$  for neutron energies 1–5 MeV and  $\pm 7\%$  for neutron energies 5–19.4 MeV). The total error was obtained by combining the contributing errors by quadratures. The absolute values of the  $Ho^{165}(n,2n)Ho^{164m}$  cross sections were obtained relative to other results<sup>8</sup> obtained at 14 MeV which had a  $\pm 9.5\%$  quoted uncertainty.

The results of the  $(n,2n)$  cross-section measurements are given in Table II and Figs. 1–5. The curves in Figs. 1–5 are theoretical cross-section predictions and will be discussed later. The measured  $(n,n')$  cross sections of  $In^{115}$  and the  $(n,\alpha)$  cross sections of  $Al^{27}$  are given in Table III and Figs. 6 and 7. The necessary  $U^{235}(n,f)$  and  $Al^{27}(n,\alpha)Na^{24}$  cross sections for fast neutrons were

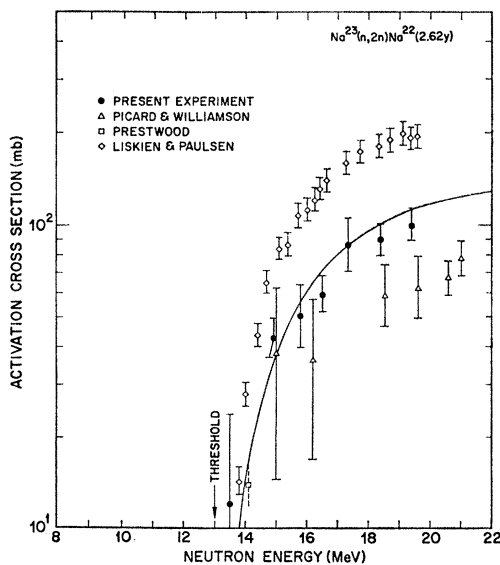


FIG. 2. The  $Na^{23}(n,2n)Na^{22}$  activation cross section. The curve corresponds to the theoretical predictions of Pearlstein and of Gardner normalized to the cross-section measurements of this experiment.

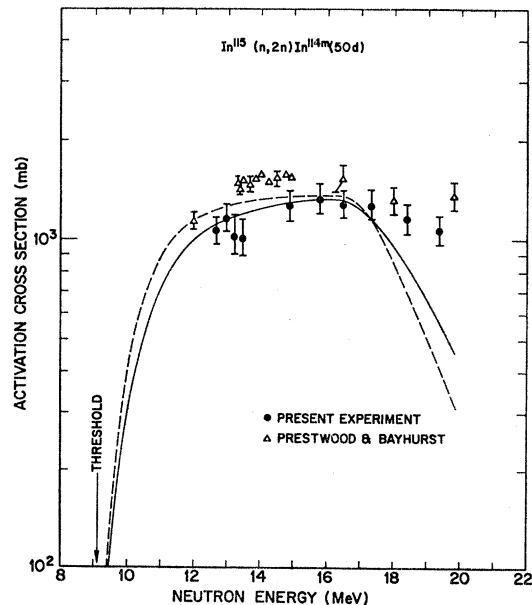


FIG. 4. The  $In^{115}(n,2n)In^{114m}$  activation cross section. The solid curve corresponds to the theoretical predictions of Pearlstein, and the dashed curve corresponds to the theoretical predictions of Gardner.

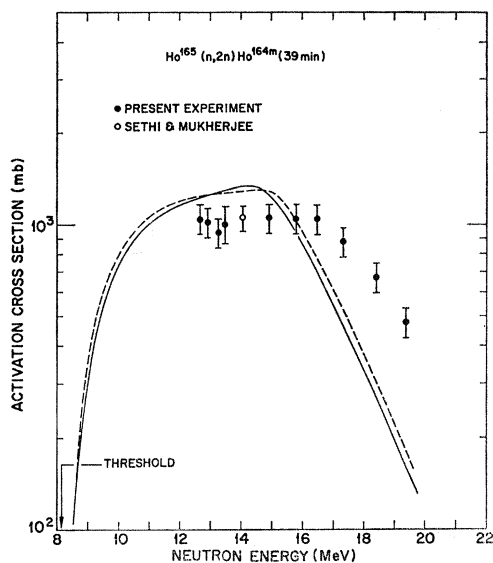


FIG. 5. The  $\text{Ho}^{165}(n,2n)\text{Ho}^{164m}$  activation cross section. The solid curve corresponds to the theoretical predictions of Pearlstein, and the dashed curve corresponds to the theoretical predictions of Gardner. The present results have been normalized to the cross-section measurement of Sethi and Mukherjee.

taken from curves in Refs. 9 and 2, respectively. The cross-section values also depend upon the thermal-neutron fission cross section<sup>10</sup> of  $\text{U}^{235}$  (577.1 b) and the thermal-activation cross section<sup>11</sup> of  $\text{Au}^{198}$  (98.8 b). Tables II and III list the average neutron energy in the laboratory system and the neutron-energy resolution corresponding to one-half the total neutron energy spread.

Figure 1 shows a comparison of the  $\text{F}^{19}(n,2n)\text{F}^{18}$  cross-section measurements of the present experiment with the results of Rayburn,<sup>12</sup> Picard and Williamson,<sup>13</sup> McCrary and Morgan,<sup>14</sup> Cevolani and Petralia,<sup>15</sup> Brill *et al.*,<sup>16</sup> Ashby *et al.*,<sup>17</sup> and Paul and Clarke.<sup>18</sup> There is excellent agreement between the present results and those of Rayburn. Also, the present results agree well with measurements of Picard and Williamson and Mc-

<sup>9</sup> *Neutron Cross Sections*, compiled by J. R. Stehn *et al.*, Brookhaven National Laboratory Report No. 325 (U. S. Government Printing and Publishing Office, Washington, D. C., 1958), 2nd ed., Suppl. 2, Vol. III.

<sup>10</sup> R. Sher and J. Felberbaum, Brookhaven National Laboratory Report No. BNL-918 (unpublished).

<sup>11</sup> *Neutron Cross Sections*, compiled by D. J. Hughes and R. B. Schwartz, Brookhaven National Laboratory Report No. 325 (U. S. Government Printing and Publishing Office, Washington, D. C., 1958), 2nd ed.

<sup>12</sup> L. A. Rayburn, *Bull. Am. Phys. Soc.* **7**, 335 (1962).

<sup>13</sup> J. D. Picard and C. F. Williamson, *J. Phys. (Paris)* **24**, 813 (1963).

<sup>14</sup> J. H. McCrary and I. L. Morgan, *Bull. Am. Phys. Soc.* **5**, 246 (1960).

<sup>15</sup> M. Cevolani and S. Petralia, *Nuovo Cimento* **26**, 1328 (1962).

<sup>16</sup> O. D. Brill, N. A. Vlasov, S. P. Kalinin, and L. S. Sokolov, *Dokl. Akad. Nauk SSSR*, **136**, 55 (1961) [English transl.: *Soviet Phys.—Doklady* **6**, 24 (1961)].

<sup>17</sup> V. J. Ashby, H. C. Catron, L. L. Newkirk, and C. J. Taylor, *Phys. Rev.* **111**, 617 (1958).

<sup>18</sup> E. B. Paul and R. L. Clarke, *Can. J. Phys.* **31**, 267 (1953).

Crary and Morgan for neutron energies greater than 14 MeV; however, for energies lower than 14 MeV the present results are somewhat lower than theirs. The results of Brill *et al.* are roughly a factor of 1.5 higher than the present results.

Figure 2 shows a comparison of the  $\text{Na}^{23}(n,2n)\text{Na}^{22}$  results of the present experiment with those of Prestwood,<sup>19</sup> Picard and Williamson,<sup>13</sup> and Liskien and Paulsen.<sup>20,21</sup> Prestwood's result of 13.8 mb at 14.1 MeV was measured relative to the  $(n,\alpha)$  cross section of  $\text{Al}^{27}$ . The quoted uncertainty of  $\pm 2.2$  mb in Prestwood's result is twice that standard deviation obtained from the reproducibility of six measurements. The present measurements fall roughly midway between the results of Picard and Williamson and the results of Liskien and Paulsen. In view of the large discrepancies in the results, the  $\gamma$ -ray counting efficiency of the crystal used in the present experiment was rechecked using a new calibrated  $\text{Na}^{22}$  source obtained from the National Bureau of Standards, and the efficiency agreed with the results of the original measurement. Since there is approximate agreement between the present measurements of the  $\text{Al}^{27}(n,\alpha)\text{Na}^{24}$  and  $\text{Mn}^{55}(n,2n)\text{Mn}^{54}$  cross sections and those of Paulsen and Liskien,<sup>22</sup> it seems unlikely that the determination of the neutron flux is involved in the discrepancy.

Figure 3 shows the present  $\text{Mn}^{55}(n,2n)\text{Mn}^{54}$  results compared with those obtained in other measurements. The results of Paulsen and Liskien<sup>22</sup> are higher than the present results by roughly 15%, which is slightly less than the combined uncertainty of the two measurements. The measurement by Weigold<sup>23</sup> of  $825 \pm 190$  mb

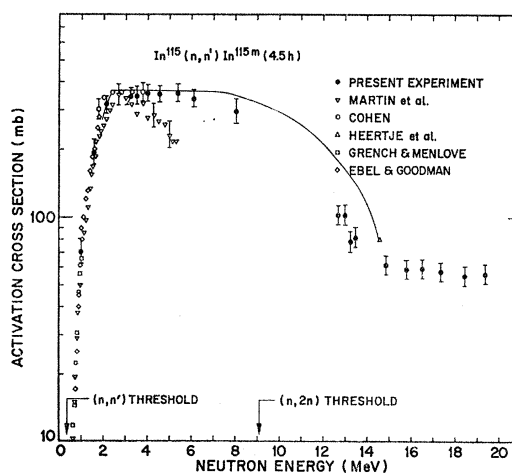


FIG. 6. The  $\text{In}^{115}(n,n')\text{In}^{115m}$  activation cross section. The curve represents the previous prediction of the cross section by Heertje *et al.*

<sup>19</sup> R. J. Prestwood, *Phys. Rev.* **98**, 47 (1955).

<sup>20</sup> H. Liskien and A. Paulsen, *Euratom Report No. EUR 119.e*, 1966, Vols. I and II (unpublished).

<sup>21</sup> H. Liskien and A. Paulsen, *Nucl. Phys.* **63**, 393 (1965).

<sup>22</sup> A. Paulsen and H. Liskien, *J. Nucl. Energy A/B* **19**, 907 (1965).

<sup>23</sup> E. Weigold, *Australian J. Phys.* **13**, 186 (1960).

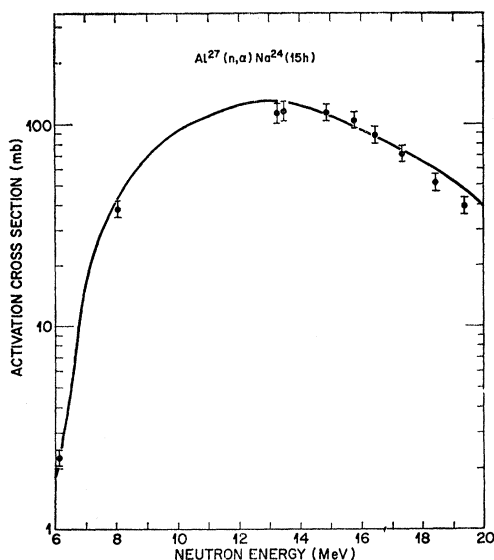


FIG. 7. The  $\text{Al}^{27}(n, \alpha)\text{Na}^{24}$  activation cross section. The curve corresponds to the average of the measurements compiled in Ref. 2.

at 14.5 MeV is in excellent agreement with the present experiment. The result of Vonach<sup>24</sup> of  $600 \pm 120$  mb at 14.1 MeV is somewhat lower than that of our experiment; however, the difference is less than the stated uncertainties. The result of Granger and Longneve<sup>25</sup> of  $1310 \pm 328$  mb at 14 MeV is considerably larger than that obtained in any of the other measurements.

Figure 4 shows the present  $(n, 2n)$  cross-section measurements on  $\text{In}^{115}$  compared with the results of Prestwood and Bayhurst.<sup>26</sup> Prestwood and Bayhurst measured their cross sections relative to the fission cross section of  $\text{U}^{238}$ ; the error bars shown on these points represent only the relative errors of their measurements. The present results are about 20% lower than the measurements of Prestwood and Bayhurst.

Figure 5 shows the present  $\text{Ho}^{165}(n, 2n)\text{Ho}^{164m}$  cross-section results. These results have been normalized to the 14-MeV value of Sethi and Mukherjee<sup>8</sup> ( $1050 \pm 100$  mb). As stated earlier, the  $\text{Ho}^{164g}$  activity was established only after the present measurements were completed. A reanalysis of the decay data has indicated that there is no definitely observable 23.9-min component in the decay of the counts in the interval between 39 and 80 keV. Any such component affects the  $\text{Ho}^{165}(n, 2n)\text{Ho}^{164m}$  cross-section values by less than 3%. No comparisons have been shown with earlier work<sup>27, 28</sup> on the  $\text{Ho}^{165}(n, 2n)\text{Ho}^{164}$  cross section since the new decay-scheme information casts doubt upon those values.

<sup>24</sup> H. Vonach, in *Symposium Physikertagung, Wien* (University of Wien, Austria, 1961), p. 67.

<sup>25</sup> B. Granger and M. Longneve, Euratom Report No. EANDC-49, 1963, p. 82 (unpublished).

<sup>26</sup> R. J. Prestwood and B. P. Bayhurst, *Phys. Rev.* **121**, 1438 (1961).

<sup>27</sup> G. C. Bonazzola, P. Brovetto, E. Chiavassa, R. Spinoglio, and A. Pasquarelli, *Nucl. Phys.* **51**, 337 (1964).

<sup>28</sup> C. S. Khurana and H. S. Hans, *Nucl. Phys.* **28**, 560 (1961).

Figure 6 shows the present results of the activation cross section for the  $\text{In}^{115}(n, n')\text{In}^{115m}$  reaction compared with the results of Ebel and Goodman,<sup>29</sup> Grench and Menlove,<sup>30</sup> Cohen,<sup>31</sup> Martin *et al.*,<sup>32</sup> and Heertje *et al.*<sup>33</sup> The results of Martin *et al.* have been lowered by 5% to correspond to the decay scheme<sup>5</sup> used in the present experiment. For neutron energies less than 3 MeV, the present results agree well with all of the other measurements. In the neutron energy range of 3 to 8 MeV the present results remain relatively flat and in line with Cohen's results, whereas, the results of Martin *et al.* decrease rapidly. Heertje *et al.* attempted to resolve this discrepancy in the cross-section shape by irradiating  $\text{In}^{115}$  with a known flux of Ra-Be neutrons and measuring the activity of the  $\text{In}^{115m}$ . According to this measurement, the cross section remains nearly constant from about 4 to 8 MeV. Beyond 8 MeV the cross section should drop off smoothly to Heertje's measurement of 80 mb at 14.6 MeV. These predictions of the cross-section shape agree very well with the present measurements. The decline in the cross-section curve for neutron energies greater than 8 MeV could be accounted for by competition from the  $(n, 2n)$  reaction, which has a threshold of 9.1 MeV.

Figure 7 shows the present cross-section measurements for the  $\text{Al}^{27}(n, \alpha)\text{Na}^{24}$  reaction compared with the curve from Ref. 2. This curve represents an average of the previous measurements of this cross section. It can be seen that there is satisfactory agreement between the present results and the average cross-section curve. The cross sections at the two highest energies fall somewhat below the curve, but the difference is less than the combined uncertainties of our results and the average cross-section curve.

The good agreement between the present measurements and the relatively well-known cross section for the  $\text{Al}^{27}(n, \alpha)\text{Na}^{24}$  reaction provides supporting evidence for the accuracy of the fission-chamber calibration, and indicates that the presence of low-energy background neutrons did not appreciably affect the present cross-section measurements for the threshold-type reactions.

#### Comparisons with Theoretical Calculations of $(n, 2n)$ Cross Sections

Recently, Barr *et al.*,<sup>34</sup> Pearlstein,<sup>3</sup> and Gardner<sup>4</sup> have calculated the energy dependence of  $(n, 2n)$  cross sec-

<sup>29</sup> A. A. Ebel and C. Goodman, *Phys. Rev.* **93**, 197 (1954).

<sup>30</sup> These values are revised from preliminary values plotted in *Neutron Cross Sections*, compiled by M. D. Goldberg *et al.*, Brookhaven National Laboratory Report No. 325 (U. S. Government Printing and Publishing Office, Washington, D. C., 1958), 2nd ed. Suppl. 2, Vol. IIB.

<sup>31</sup> S. G. Cohen, *Nature* **161**, 475 (1948).

<sup>32</sup> H. C. Martin, B. C. Diven, and R. F. Taschek, *Phys. Rev.* **93**, 199 (1954).

<sup>33</sup> I. Heertje, W. Nagel, and A. H. W. Aten, Jr., *Physica* **30**, 775 (1964).

<sup>34</sup> D. W. Barr, C. I. Browne, and J. S. Gilmore, *Phys. Rev.* **123**, 859 (1961).

tions using a statistical-model approach. The procedure presented by Pearlstein closely follows the semiempirical approach used by Barr *et al.*; however, the model was extended by Pearlstein to include competition from  $(n,3n)$  reactions, and the level-density parameter was changed to reflect the shell characteristics of the nucleus. Gardner followed a procedure somewhat similar to that used by Pearlstein to obtain an expression for  $(n,2n)$  cross sections. However, Gardner used a different expression for the level-density parameter, and he did not use the same function to compensate for charged-particle emission.

Figures 1–5 show the  $(n,2n)$  cross-section results of the present experiment compared with the theoretical predictions of Pearlstein<sup>3</sup> and of Gardner.<sup>4</sup> The solid curves correspond to Pearlstein's  $(n,2n)$  cross-section predictions [Eq. (6), Ref. 3], and the dashed curves correspond to Gardner's predictions [Eq. (6), Ref. 4]. The semiempirical theory of Pearlstein is not necessarily valid for nuclides with mass number  $A < 30$  because of discontinuities in his competition ratio. Similarly, Gardner's normalizing function is not necessarily valid for proton numbers  $Z < 30$ . In view of this, the theoretical curves for  $F^{19}$  and  $Na^{23}$  have been normalized to the results of the present measurements. Only one curve is shown for  $F^{19}$  and one for  $Na^{23}$  since the two calculated curves very nearly coincided after normalization. For these two nuclides, the shapes of the theoretical curves agree reasonably well with the measured cross section. The calculated curves for  $Mn^{55}$  shown in Fig. 3 were not normalized to the measurements. Since the  $In^{115}$  and  $Ho^{165}$  theoretical predictions of Pearlstein or Gardner include production of  $In^{116g}$  and  $Ho^{166g}$ , these predictions have been lowered to correspond to production of the metastable states only. The  $In^{115}$ - $(n,2n)^{114g}$  cross section<sup>35</sup> at 14.8 MeV is  $360 \pm 40$  mb. When this is combined with our 14.96-MeV value for  $In^{114m}$ , a normalization factor of 0.78 results for the theoretical predictions. This factor has been applied to all of the energies. Similarly, since there was an isomer-

ratio measurement<sup>8</sup> at 14 MeV for  $Ho^{165}(n,2n)^{164m,g}$ , the theoretical curves have been renormalized by a factor of 0.59 to correspond to production of  $Ho^{164m}$  only. The magnitudes of the theoretical calculations are in good agreement with the experimental results; however, for  $In^{115}$  and  $Ho^{165}$  the theoretical curves start to decrease at a lower energy than the experimental results. This decrease in the calculated cross section is caused by competition from the  $(n,3n)$  reaction. This discrepancy between the calculations and the measurements could be caused by an overestimation of the  $(n,3n)$  cross sections in the theory. Possibly, the assumption that multiple emission of the highest order takes place if energetically possible is not valid for neutron energies above the  $(n,3n)$  reaction thresholds. In addition, the occurrence of the reaction by a direct-interaction process would tend to give a discrepancy of this type. Finally, there is some uncertainty in the energy of the thresholds for the  $(n,3n)$  reactions; however, it would not appear from binding-energy measurements<sup>36</sup> that this uncertainty is large enough to account for the discrepancy.

Pearlstein fitted his calculated  $(n,2n)$  cross sections to the experimental data for several nuclides, and he also observed that at high energies, where competition from the  $(n,3n)$  reaction is important, his model often underestimated the cross section.

The calculated cross sections of Pearlstein and of Gardner are similar in shape and magnitude. Gardner's cross-section curve rises from threshold energy somewhat more sharply than does Pearlstein's; however, the two curves never separate from each other by more than 25% in the energy range of the present experiments. The accuracy of the present cross-section measurements is insufficient to conclude that one method of calculation is superior to the other. Gardner's "normalization function" seems equivalent to Pearlstein's "competition ratio." The same empirically determined nonelastic cross-section function<sup>37</sup> was used for both sets of calculations.

<sup>35</sup> J. H. E. Mattauch, W. Thiele, and A. Wapstra, Nucl. Phys. **67**, 32 (1965).

<sup>36</sup> R. Prasad, D. C. Sarkar, and C. S. Khurana, Nucl. Phys. **88**, 349 (1966).

<sup>37</sup> N. N. Flerov and V. M. Talyzin, J. Nucl. Energy **4**, 529 (1957).